Toxicology and Applied Pharmacology 466 (2023) 116470

Contents lists available at ScienceDirect

Toxicology and Applied Pharmacology

journal homepage: www.elsevier.com/locate/taap

AR13 peptide-conjugated liposomes improve the antitumor efficacy of doxorubicin in mice bearing C26 colon carcinoma; *in silico, in vitro,* and *in vivo* study

Atefeh Biabangard [a], Ahmad Asoodeh [a,*], Mahmoud Reza Jaafari [b,c,*], Fatemeh Moosavi Baigi [a]

[a] Department of Chemistry, Faculty of Science, Ferdowsi University of Mashhad, Mashhad, Iran
[b] Nanotechnology Research Center, Pharmaceutical Technology Institute, School of Pharmacy, Mashhad University of Medical Sciences, Mashhad, Iran
[c] Department of Pharmaceutical Nanotechnology, School of Pharmacy, Mashhad University of Medical Sciences, Mashhad, Iran

ARTICLE INFO

Editor: Lawrence Lash

Keywords:
AR13 peptide
Colon cancer
Drug delivery
PEGylated liposomal doxorubicin
Target therapy

ABSTRACT

Currently, liposomes have emerged as efficient and safer nano-carriers for targeted therapy in different cancers. This work aimed to employ PEGylated liposomal doxorubicin (Doxil®/PLD), modified with AR13 peptide, to target Muc1 on the surface of colon cancerous cells.

We performed molecular docking and simulation studies (using Gromacs package) of AR13 peptide against Muc1 to analyze and visualize the peptide-Muc1 binding combination. For *in vitro* analysis, the AR13 peptide was post–inserted into Doxil® and verified by TLC, ^{1}H NMR, and HPLC techniques. The zeta potential, TEM, release, cell uptake, competition assay, and cytotoxicity studies were performed. *In vivo* antitumor activities and survival analysis on mice bearing C26 colon carcinoma were studied.

Results showed that after 100 ns simulation, a stable complex between AR13 and Muc1 formed, and molecular dynamics analysis confirmed this interaction. *In vitro* analysis demonstrated significant enhancement of cellular binding and cell uptake.

The results of *in vivo* study on BALB/c mice bearing C26 colon carcinoma, revealed an extended survival time to 44 days and higher tumor growth inhibition compared to Doxil®. Thus, the AR13 peptide could be explored as a potent ligand for Muc1, improving therapeutic antitumor efficiency in colon cancer cells.

1. Introduction

Nowadays, drug delivery technology has gained widespread attention due to its tremendous potential application for treating various types of diseases. In addition, selecting the right carrier that is biocompatible, nontoxic, and has the provision for drug-controlled release is a crucial aspect of this approach (Rajagopalan and Yakhmi, 2017). In order to efficiently and selectively deliver the drug to the desired therapeutic tissue (targeted drug delivery), nanoparticles (NP) as Nano-carriers are employed. Liposomes and micelles are the first generation of nanoscale-size particles in the Drug Delivery System (DDS) that have received FDA approval (Lee, 2019; Shi et al., 2008). To increase the circulating time and hydrophilicity of liposomes, sometimes polyethylene glycol (PEG) molecules are attached to their surface (Maiti and Sen, 2017). One of the well-known liposomal formulations is PEGygated liposomal doxorubicin (PLD, Doxil®, or Caelyx®), which has the stable remote loading of doxorubicin (Dox) (Barenholz, 2012). High-efficiency and accurate targeting effects are achieved by incorporating targeting ligands (such as antibodies, aptamers, glycoproteins, peptides, or vitamins) to the surface of liposomes or PLDs (Sonju et al., 2021). Targeting ligands could recognize and bind to target receptors overexpressed on the surface of particular cells or tissue components (Yoo et al., 2019).

In this study, we targeted Mucin1 (Muc1), which is known to be overexpressed on the surface of colon cancer and breast cancer cells (Taylor-Papadimitriou et al., 1999). Muc1 is a structural and glycosylated membranous bound mucin consisting of three different domains: an extracellular domain (Muc1 C-terminal subunit; 58 amino acids (aa)), a transmembrane domain (Muc1-N; 28 aa), and a cytoplasmic tail (72 aa). The extra-domain of Muc1 consists of numerous tandem repeat amino acids (called VNTR). It has been reported that the Muc1 protein might be a potential factor in cancer metastasis and is involved in cell-

* Corresponding authors.
E-mail addresses: asoodeh@um.ac.ir (A. Asoodeh), jafarimr@mums.ac.ir (M.R. Jaafari).

https://doi.org/10.1016/j.taap.2023.116470
Received 4 December 2022; Received in revised form 11 March 2023; Accepted 13 March 2023
Available online 17 March 2023

extracellular matrix interactions and tumor progression (Agrawal et al., 2018). Therefore, it could be considered a crucial key factor in cancer treatment. Our previous experimental study demonstrated that targeted liposomes with an antimicrobial peptide could improve the antitumor efficiency of doxorubicin and increase the lifespan of mice bearing colon carcinoma. (Biabangard et al., 2022). This study aimed to evaluate the targeting capacity and antitumor efficiency of liposomal doxorubicin modified with a different number of peptides. For this purpose, we used AR13 peptide (AQQLAAQLPAMCR) as a ligand to target Muc1 on the apical surface of colon cancer cells. AR13 is an angiotensin-converting enzyme (ACE) inhibitory peptide, released from the trypsin hydrolysate of wheat gluten protein (Darban et al., 2017b; Asoodeh et al., 2014). Among the different peptides in our peptide bank, AR13 had the most favorable physicochemical characteristics, and hence it was selected as a ligand for our analysis. Therefore, PLD was conjugated with AR13 peptide (called Muc1-targeted liposomes) to target Muc1. The dynamic molecular simulation was conducted to verify this interaction between the Muc1 and AR13 peptides. Also, the *in vitro* studies (cell binding affinity and cellular uptake, and cytotoxicity MTT assay) were carried out. Besides, *in vivo* analysis were performed on BALB/c mice bearing C26 colon carcinoma.

2. Materials and methods

2.1. Materials

AR13 peptide (AQQLAAQLPAMCR) was chemically synthesized by GL Biochem (Shanghai, China) with 95% purity. DSPE-PEG2000-maleimide was purchased from Avanti Polar Lipids (Alabaster, AL). MTT 3-(4, 5-dimethylthiazol-2-yl)-2, 5-diphenyltetrazolium bromide was obtained from Sigma (Aldrich, Germany). RPMI 1640 culture medium and fetal bovine serum (FBS) were obtained from Gibco (Carlsbad, CA). Isopropanol, chloroform, N-Hydroxysulfosuccinimide (Sulfo-NHS; ≥98%), and N-(3-Dimethylaminopropyl)-N′- Ethyl-3-(3-Dimethylaminopropyl) carbodiimide (EDC; ≥99.0%) were purchased from Merck (Darmstadt, Germany). PLD (Doxil®) was obtained from Behestan Darou Company (Tehran, Iran).

2.2. Computational study

2.2.1. Preparation of the structures

In this study, the AR13 peptide was selected as a ligand, and the Muc1 protein as a receptor. The crystal structure of Muc1 VNTR domain (PDBID: 1SM3) was obtained from the RCSB protein data bank (https://www.rcsb.org). All structural-based modifications were conducted, and missing residues were added by the Discovery studio client 4.5 (Accelrys, Inc. San Diego, CA). AR13 peptide structure was predicted using the PEP-FOLD3 server (https://bioserv.rpbs.univ-paris-diderot.fr/services/PEP-FOLD3). The 3D-modelled structures were energy-minimized by Chem3D (MM2 10,000 iterations and minimum RMS gradient of 0.01). Consequently, the evaluation of the model was performed using the PROCHECK server (Laskowski et al., 1996).

2.2.2. Molecular docking studies

Molecular Docking analyses of ligand-receptor were performed using the Patch Dock web server (Muc1 VNTR domain as a receptor with AR13 peptide) [Schneidman-Duhovny et al., 2005; Khondee et al., 2018]. Afterward, Patch Dock results were refined using Fast Interaction Refinement Molecular Docking server (FIRE DOCK). The Discover Studio client and PyMOL were used for visualizations and renderings.

2.2.3. Molecular dynamic simulation

The docking complex was selected for further MD simulations (Swope et al., 2006). Simulations were conducted using the GROMACS 5.1.1 package with the GROMOS96 43a1 force field. First, the peptide-protein complex was embedded into a TIP3P water cubic box with a distance of 10 Å between the protein and the box edge. In order to neutralize the system, the chloride ion (Cl^-) was added. Particle Mesh Ewald (PME) method (Nam et al., 2005) and SHAKE algorithm (Ryckaert et al., 1977) were applied to all bounds. In all directions, periodic boundary conditions were used during the simulation. First, the system was subjected to the descent energy minimization and set to the maximum of 1000 kJ/(mol•nm). After 50,000 steps of minimization, the system was equilibrated at 100 ps under a constant volume ensemble (NVT) with a position restraint on all water oxygen. The time step for the simulation was set to 2 fs. Subsequently, constant pressure simulations (NPT) were run for 1 ns and maintained at 300 K and a pressure of 1 bar. Finally, the system was simulated (without positional constraints) for 100 ns ($T = 300$ K and $P = 1$ bar). All covalent bonds to hydrogen atoms were constrained using the default linear constraint solver (LINCS) algorithm (Hess et al., 1997).

2.3. Liposome preparation

2.3.1. Conjugation of peptide to DSPE-PEG2000-maleimide

The reaction between the sulfhydryl group (SH) of cysteine (Cys_{12} of AR13) and maleimide was performed in chloroform and the DSPE-PEG2000-maleimide solution. Then, the AR13 peptide was dissolved in DMSO (in a 1:1.2 ratio) and stirred overnight at room temperature.

2.3.2. Verification of peptides conjugation

The TLC, HPLC, and ^{1}HNMR methods were conducted to confirm the conjugation of AR13 peptide to the lipid. Thin layer chromatography (TLC) was performed with a developing solvent of chloroform/methanol/water (90/10/2) after exposure to iodine vapor. High-Performance Liquid Chromatography (HPLC) was performed using a C8 column (10 × 250 mm, manufactured by Machereye Nagel GmbH & Co. Duren, Germany) and a UV detector set at 214 nm at a flow rate of 1 ml/min. A mixture of solution A (0.1% TFA + distilled water) and solution B (0.098% TFA + acetonitrile) was used for elution (injection volume: 20 μL). The ^{1}H NMR spectra of the samples were recorded on a Bruker Avance 300 MHz instrument. NMR samples were prepared by dissolving each in DMSO (20 mg/ml).

2.3.3. Post insertion

The post-insertion method (Darban et al., 2017a; Moreira et al., 2002) was conducted to modify PLD with AR13 peptide. Briefly, DSPE-PEG2000-AR13 micelles were added to 2 ml of PLD, and the liposomal suspension was incubated for 1 h at 65 °C. AR13-PLD formulations were obtained by inserting a proper number of AR13 peptides on the surface of each liposome (50, 100, 200, and 400) (additional data are given in supplementary data). The phospholipid content of preparations was measured using a method based on the Bartlette phosphate assay (Bartlett, 1959).

2.3.4. Characterization of liposomes

Particle size, polydispersity index (PDI), and zeta potential of these modified liposomes were measured by Dynamic Light Scattering (Nano-ZS; Malvern, UK) in dextrose (5%) at room temperature (Clogston and Patri, 2011). For this purpose, diluted liposomal suspension in dextrose buffer was added to the sample cuvette, placed in zeta sizer and stabilized for 2 min. The average particle size was determined by performing the experiments in triplicate.

The morphology of liposomes was visualized with the transmission electron microscope (TEM) (Zeiss, Jena, German). Dox loading efficiency was determined by fluorimetry (Perkin-Elmer LS-45, US) (ex: 485 nm and em: 590 nm) using a serial dilution of Dox as a standard. So, 1 ml of each formulation was dissolved in 9 ml of acidified isopropyl alcohol. Then, the mixture was incubated at 70 °C for 10 min. The test was done in triplicate. The efficiency of encapsulation was assessed by the following formula (Hayat et al., 2020):

$$\text{Dox encapsulated } (\%) = \frac{\text{Dox concentration after purification}}{\text{Dox concentration before purification}} \times 100$$

2.4. Release study

The release profile of Dox from modified PLDs was studied in plasma-like media (Shahraki et al., 2021). For this purpose, 1 ml of each formulation was mixed with 9 ml of release media (5% dextrose containing 50% FBS) and incubated at 37 °C at pH 7.4. At various time points (0, 1, 2, 4, 6, 12, and 24 h), 1 ml of samples was taken and then incubated with Dowex® resin. Dox concentration was obtained using a spectrofluorometer (LS-45, Perkin–Elmer, USA).

Dox released was then calculated using the following equation (Haghiralsadat et al., 2018):

$$\text{Release } (\%) = 1 - \frac{\text{Dox concentration at time t}}{\text{Dox concertation at the time 0}} \times 100$$

2.5. Cellular studies

2.5.1. Cell culture

HUVEC (human umbilical vein endothelial cell) as the control group and C26 colon carcinoma cell lines were purchased from Pasteur Institute (Tehran, Iran). RPMI 1640 medium (Euroclone) supplemented with 10% fetal bovine serum (FBS, heat-inactivated, Gibco), 100 unit/mL penicillin, and 100 mg/mL streptomycin (Sigma). All cell lines were incubated in a 5% CO_2/ 95% air-humidified atmosphere at 37 °C.

2.5.2. Cell uptake study

Cellular binding and uptake of ligand-targeted formulations were studied at 4 °C and 37 °C, respectively (Mashreghi et al., 2020; Moosavian et al., 2018). Two cell lines, HUWEC and C26, were seeded in each well of 6-well plates (2×10^5 cells/well). After overnight incubation at 37 °C, formulations were added to the cells and treated for 3 h at 4 °C and 37 °C. After washing with PBS and detaching by trypsin, acidified isopropanol was added to each well and incubated overnight. Then, cells were centrifuged (1500 rpm/ 5 min) and assayed using flow cytometry (BD Biosciences, USA).

2.5.3. Competition assay

The competition binding assay was performed to examine the specificity and ability of the AR13-PLD to bind to Muc1 receptor (Arabi et al., 2015). C26 cells were incubated with 2 μg/mL of free AR13 peptide, in the absence of AR13-PLD formulations as a competing agent, at 37 °C for 0.5 h. After that, AR13-PLD formulations were added for another 1 h. Then, after centrifugation of the cells (1500 rpm/5 min), the fluorescence signal was read using BD-FACSCalibur in the FL2 channel.

2.5.4. Cytotoxicity assay

The MTT test was conducted to analyze the IC_{50} (the concentration required for 50% inhibition of cellular growth) value of formulations *in vitro* (Korani et al., 2020). Two cell lines, C26 and HUWEC (as control), were seeded in 96-well plates at a density of 5000 cells per well and were incubated at 37 °C overnight.

Then, cells were treated with liposomal formulations and PLD (in FBS-free medium) in triplicate and were incubated for 1, 3, and 6 h at 37 °C. After washing cells, they were re-incubated for 72 h. MTT was added, and after 4 h, the absorbance of cells was evaluated at 545 nm against a background of 630 nm by Stat-Fax 2100 microplate reader (Awareness Technology Inc. USA). Assay was performed twice for each cell line. IC_{50} data were obtained using the CalcuSyn version 2 software (BIOSOFT, UK).

2.6. Animal study

2.6.1. Biodistribution

Female BALB/c mice (4–5 weeks, 17–21 g) were purchased from the Pasteur Institute of Iran ($n = 25$) and kept in groups including PLD-50, PLD-100, PLD-200, PLD 400, PLD, and PBS (as a control group) ($n = 5$ per each group). For the biodistribution study (Nikoofal-Sahlabadi et al., 2018), 3×10^5 C26 tumor cells were injected subcutaneously into the mice. After 14 days, mice were treated intravenously with formulations (15 mg/kg). The control group received 100 μL of PBS. Following this, the blood samples were collected from the retro-orbital sinus after 3, 12, 48, and 72 h to analyze the drug release rate in the blood circulation.

The blood samples were centrifuged (14,000 rpm/ 10 min), and the fluorescence intensity of formulations was measured by spectrofluorimetry (Perkin-Elmer LS-45) at λ Ex/Em = 480/590 nm. Then, 72 h after the administration of formulations, the mice were anesthetized with a solution of ketamine (100 mg/kg) and xylazine. All organs (muscle, liver, kidney, spleen, and heart) of the mice and the tumor were removed. These tissues were harvested, weighed, and homogenized in acidified isopropanol using zirconia beads by Mini-Beadbeater-1 (Biospec, OK). Samples were stored in 80% (*v*/v) isopropyl alcohol at 4 °C overnight. Subsequently, samples were centrifuged (14,000 rpm, 10 min), and their supernatant absorbance was determined at the wavelengths mentioned above (Moosavian et al., 2018).

2.6.2. Antitumor and survival analysis

The body weight and tumor volume of animals were monitored for 44 days. An experimental growth tumor curve was obtained by measuring tumor dimensions using a caliper as follows (Turkbey et al., 2012): Tumor Volume = 0.5 × Length × Height × Width.

Considering ethical aspects, mice were euthanized when the tumor volume reached above 1000 mm^3 or body weight loss was >20%. In this study, the experimental protocols were approved by the Ethics committee of Ferdowsi University of Mashhad (Ethics number: IR.UM.REC.1400.362).

2.7. Statistical analysis

Data analysis was performed using GraphPad Prism 6.0 (Graph-Pad software, Inc., San Diego, CA, USA). To assay, the statistical differences between the groups, a one-way analysis of variance (ANOVA) was employed. Survival analysis was performed by the Kaplan-Meier method and analyzed by the log-rank test (Goel et al., 2010). Data are presented as mean ± SEM (standard error of the mean) of at least twice independent experiments.

3. Results and discussion

In the last couple of decades, liposomes have gained much attention as a drug delivery system in clinical uses (Kim, 2016). PEGylated liposomal doxorubicin, PLD or Doxil®, is the first FDA-approved and EPR-based nanoparticle drug that has shown promising therapeutic efficacy as an antitumor agent (Subhan et al., 2021; Barenholz, 2012). Here, we conjugated a peptide (AR13) as a targeting ligand to the surface of PLD to target Muc1 protein on the apical membrane of colon cancer cells. Thus, the accumulation of AR13-PLDs around the tumor site leads to the delivery of Dox specifically to colon cancer cells through the active targeting (Amin et al., 2013).

3.1. Structural properties and validation

AR13 peptide with the following sequence: AQQLAAQLPAMCR, has a molecular weight of 1400.68 g/m, the net charge of 1 (at pH 7), and a PI of 8.92. Validation of the AR13 peptide structure was determined by Ramachandran plot (Ramakrishnan and Ramachandran, 1965) (using Procheck server) as follows: Number of residues in the favored region:

100%, Number of residues in the disallowed region: 0%, and G-Factor was −0.16. The G-factor of the model indicates a value > −0.5. Accordingly, the structure has a good stereo-chemical quality.

3.2. Molecular docking study

Molecular docking analysis using Pack and refinement by Fire dock revealed the binding energy of −21.67 (kcal/mol) and hydrogen bound energy of −2.82 (kcal/mol). The maximum number of H-bond was about 4. According to the docking results, the AR13 peptide can bind effectively to the Muc1 target protein.

Molecular dynamics (MD) simulations constitute the essential tools for the algorithmic exploration of ligand binding mechanisms of action (Swope et al., 2006). The complex of receptor/ligand is illustrated in Fig. 1a. Here, to analyze the stability of the system backbone, RMSD (root mean square deviations) was evaluated after 100 ns (Fig. 1b). Furthermore, the results of the Radius of gyration (Rg), a measure of structural compactness and stability of a protein (Zhiping et al., 1992), confirmed this (Fig. 1c). The system reached an equilibrated dynamical state of relatively around 56 ns. It was indicated that Rg values revealed the variation during the simulation time (Neto et al., 2022). Our system demonstrated Rg values of around 0.8 Å during simulation. With this in mind, our system suggests conformational stability of ligand (AR13) and receptor (Muc1) over the 100 ns. RMSF (root mean square fluctuation) was calculated to represent the atom movement of the AR13 peptide and Muc1 during 100 ns (Fig. 1d). RMSF profile of AR13 backbone showed conformational fluctuations of residues 2 and 5 (Qln and Ala). The intramolecular hydrogen bonding (H-bonding) between the Ala-6 and Ala-10, Ala-1 and Leu-4, Ala-10, and Qln-7 stabilized these residues of AR13 and thus reduced their fluctuation. However, Qln-2 and Ala-5, which take part less in H-bonding, have more RMSF values. The different number of H-bond interactions between the peptide and Muc1 (from 1 to 9) is depicted in Fig. 1e.

3.3. Characterization

In the present study, we conjugated the carboxylic group of DSPE-PEG2000-Maleimide with AR13 (SH of Cys) peptide *via* thioether

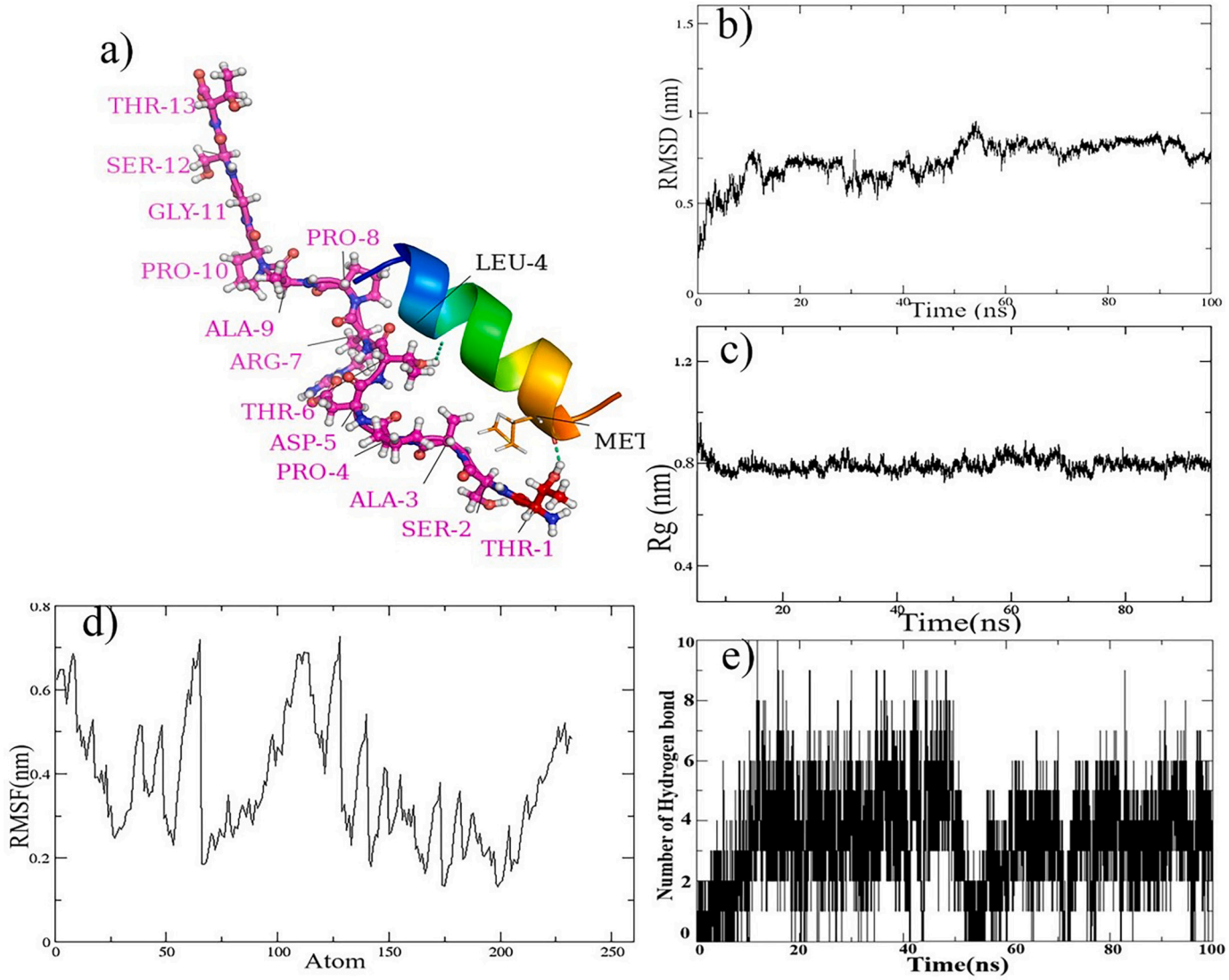

Fig. 1. MD simulation analysis of AR13- Muc1 complex after 100 ns simulation. (a) 3D structure of the complex. Side view of Muc1 (Stick) and AR13 (Cartoon) was shown. The green dashed lines are the H-bonds. (b) The root means square deviation (RMSD) plots of the protein and ligand backbone atoms for the selected systems (Muc1-AR13). (c) Variation of Radius of gyration (Rg), (d) RMSF graph of the Cα backbone atoms for the AR13 peptide, and (e) the total number of hydrogen bonds formed throughout the100 ns MD simulation. (For interpretation of the references to colour in this figure legend, the reader is referred to the web version of this article.)

bonding. Fig. 2a shows the ^{1}H NMR (in DMSO) spectrum of the lipid-peptide complex and corresponding labeled peaks. DSPE-PEG2000-AR13 was synthesized by the SH-groups conjugated to the Maleimide of DSPE-PEG2000-Mal. The peak at 3.6 ppm corresponded to the PEG resonance (Diao et al., 2019), indicating the existence of a hydrophilic PEG long-chain. The peak of DSPE groups was located at~1.1 ppm (Pinheiro et al., 2020), and the peaks for the AR13 peptide were observed around 6–7.5 ppm. As a result, the presence of these peaks in the DSPE-PEG2000-AR13 diagram confirmed the successful conjugation of AR13 to the DSPE-PEG2000-Mal lipid.

RP-HPLC results of the free peptides and the conjugated peptide are depicted in Fig. 2 b. The peak area in RP-HPLC chromatograms of free AR13 was larger (retention time, 5.5 min) than the peptide-lipid conjugate peak (DSPE-PEG2000-AR13). The results revealed an almost complete reaction (around 100%) between the maleimide group and the SH group of the AR13 peptide. On the TLC (Fig. 2c), the disappearance of the DSPE-PEG2000-Mal spot demonstrates the conjugation of AR13 peptide. From these results, the conjugation of AR13 peptide to DSPE-PEG2000-Mal lipid was confirmed. Conjugation of peptides *via* thioether linkage to delivery vectors has been realized in several studies (Liang et al., 2018; Reinhardt and Neundorf, 2016). This conjugation could functionalize peptides and liposomes. Additionally, compared to cleavable linkers, covalently bound linkers like thioether linkers are more stable in circulation. These linkers may further improve the antitumor efficiency of cytotoxic drugs (Nolting, 2013).

The morphology of PLD and PLD-100 was obtained with a Transmission Electron Microscope (TEM) following negative staining by phosphotungstic acid. TEM analysis (Fig. 2d & e) demonstrated the spherical shape of PLD-100 and PLD formulations (≈100 nm) and was consistent with the results of DLS. Other studies have shown that spherical nanoparticles ranging from 50 to 200 nm are suitable for tumor targeting (Subhan et al., 2021). Hence, our formulations are in a reasonable range.

For the preparation of liposomal formulation, the post-insertion method is a rapid and effective technique in clinical use (Iden and Allen, 2001). The total number of phospholipids in the liposomal formulation investigated by phosphate assay was 6 mM. Accordingly, as we knew the number of liposomes in each milliliter (nearly 10^{14}) (Haftcheshmeh et al., 2021), we achieved 50, 100, 200, and 400 peptides on the surface of any individual PLD (supplementary data).

The physicochemical characterization of the formulations showed excellent properties (Table 1) since the encapsulation efficiencies of approximately all formulations were above 90%. This feature indicates the successful post-insertion, which had a negligible effect on liposome size (PDI <0.2). It should be noted that the slight increase in the liposome size contributed to the conjugation of different numbers of peptides on the surface of liposomes.

3.4. Release study

The *in vitro* release behavior of formulations was studied for 24 h. It was indicated that PLD-400 and PLD-50 formulations had the most and least release behavior, respectively (Fig. 3a). This slightly higher Dox release of PLD-400 might be due to its larger size (Nagayasu et al., 1999). It was investigated that smaller liposomes encapsulated antitumor drugs could release the drug more readily into the bloodstream. However, the drug release from liposomes is mostly affected by lipid composition rather than by liposome size. Moreover, the presence of cholesterol, rigid phospholipids, and DSPC (1,2-distearoyl-sn-glycero-3-phosphocholine) in liposomal membranes caused a decrease in the release of drugs from liposomes (Hernández-Caselles et al., 1993). Here, the size and composition of our liposomal formulations were optimal, and the release profiles of all formulations were <10%. Altogether, AR13 peptide conjugation had no significant effect on the leakage stability of PLD formulations.

3.5. In vitro cytotoxicity studies

MTT assay was performed to determine the cytotoxicity of Dox, PLD, and other formulations (PLD-50, PLD-100, PLD-200, and PLD-400) *in vitro*. The IC_{50} values are depicted in Fig. 3b & c. It was revealed that the IC_{50} values of PLD in C26 cells were higher than the IC_{50} values of other formulations. AR13-PLD formulations had higher cytotoxicity (lower IC_{50}) than non-modified liposome (PLD) which could be as a result of the greater uptake of formulations by the C26 cells. Mainly, after 9 h incubation, the IC_{50} values of AR13-PLDs exhibited more decrease compared to PLD, although it wasn't significant. Since HUVEC cells are non-tumor cells, they displayed a reduced response than C26 cancer cells (Fig. 3c). Thereby, nano-liposomal formulations aren't cytotoxic toward normal cells. Meanwhile, the cytotoxicity of the free drug (Dox) is considerably higher than other PLD formulations. These results are in good agreement with previous studies which have highlighted the role of active targeting in cytotoxicity of targeted liposomes compared to non-targeted liposomes (PLD) (Bolat et al., 2021; Arabi et al., 2015).

3.6. Cellular binding and uptake

A comparison of the Geometric mean fluorescence (MFI) of the C26 cells treated with AR13-PLDs and the representative histogram is displayed in Fig. 4. As indicated, all targeted formulations exhibited considerably significant enhancement in liposomal uptake by C26 cells compared to PLD at 4 °C (Fig. 4a & b) and 37 °C (Fig. 4c & d) ($p < 0.0001$).

It is noted that nanoparticles with positive charge have a higher rate of cellular uptake and nonspecific internalization than neutral or negatively charged formulations (Alexis et al., 2008). Other studies also proved that the presence of peptides, aptamers, or other molecules on the surface of liposomes (modified liposomes) could increase the rate of internalization into the cells and cause more cytotoxicity compared to liposomes without any targeted molecules (Mashreghi et al., 2020).

When C26 cells were treated with the free peptide before the incubation with AR13-PLD, MFI values, as an indicator of cell uptake of formulations, decreased mainly due to the competition between free peptide and the AR13-PLD for the same binding site (Muc1 receptor). Therefore, no shift in the histogram and no significant difference in cellular uptake were observed (Fig. 4 e & f). These results showed that AR13-PLD could enhance target specificity and that AR13 peptide has a favorable affinity to C26 cells.

3.7. Biodistribution

The concentration of the Dox fluorescence intensity in the blood (after injection of 15 mg/kg of AR13-PLD formulations in mice bearing subcutaneous C26 colon cancer tumors) is shown in Fig. 5a. It is indicated that even after 72 h of injections, there were significant differences between PLD-50, PLD-200, PLD-400, and PLD. As demonstrated, PLD had the most concentrations at different times in that the conjugation of the peptide with a positive charge on the surface of liposomes could slightly decrease the circulation time (Hatakeyama et al., 2013).

To identify the drug distribution in the heart, spleen, lung, liver, kidney, and tumor, the Dox fluorescence intensity of each formulation was evaluated by fluorimetry (Fig. 5b). In the heart, lung, and kidney, the accumulation of AR13-PLD formulations was very low and was not statistically significant. At the tumor site, AR13 formulations revealed a high accumulation level compared to PLD, which might be due to the efficiency of active targeting with the AR13 peptide or EPR (Enhanced permeability and retention) effect. Leaky tumor microvasculature and higher vascular permeability in the solid tumor might lead to the accumulation of liposomes with an appropriate size and charge at the target tissue (Fukumura and Jain, 2007). Accumulation of PLD-50 and PLD-100 in the liver and tumor was statistically significant compared with PLD. Other literature also reported that PEG liposomes had a higher

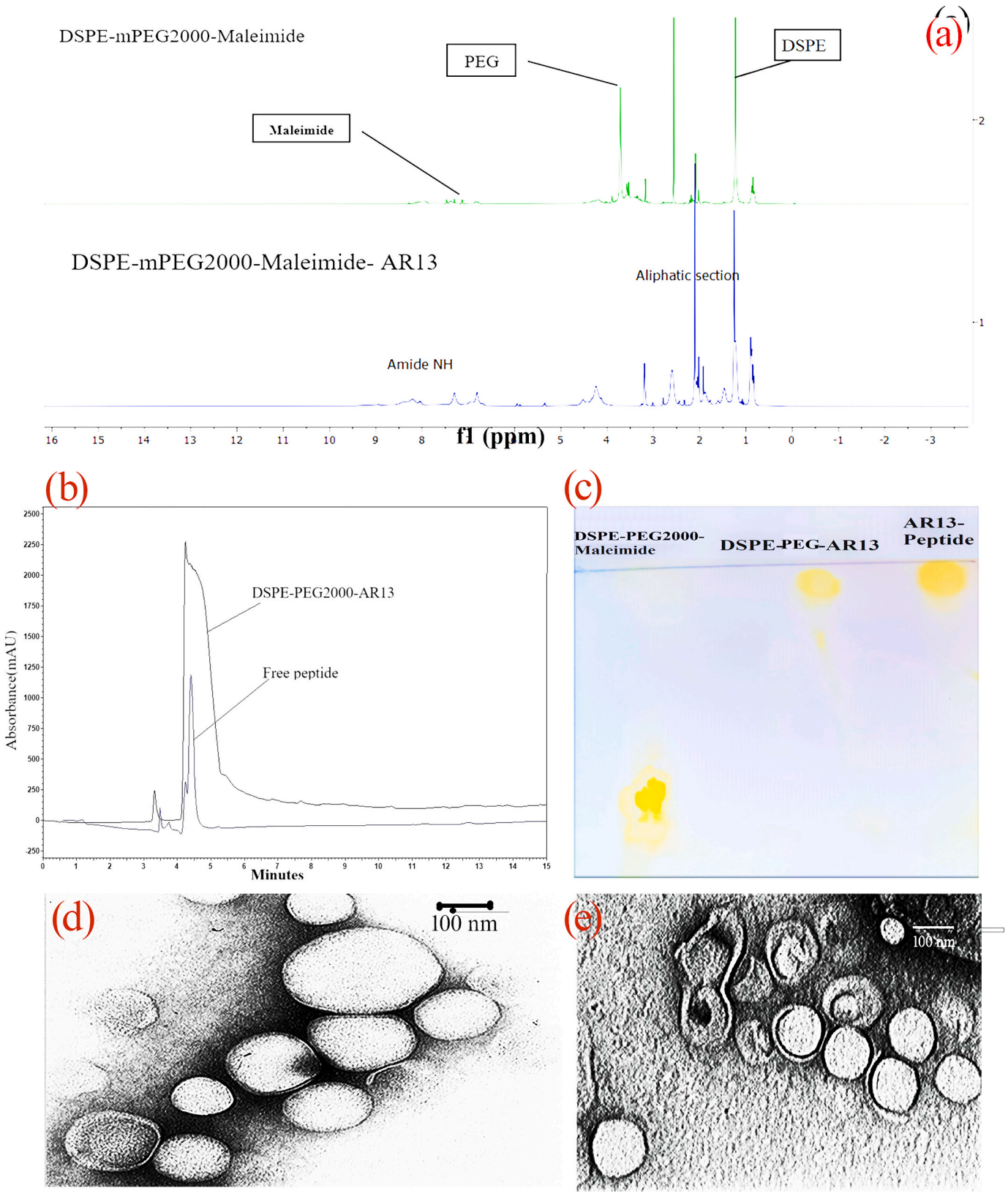

Fig. 2. Confirmation of conjugation between AR13 peptide and DSPE-PEG-Maleimide by using ^{1}H NMR (a), Reverse phase HPLC of AR13 peptide and DSPE-PEG2000-AR13(b), and TLC (c). TEM images of PLD (d) and PLD-100 (e) (negative staining with phosphotungstic acid).

Table 1
Physicochemical characteristics of formulations. Each value represents as mean ± SD ($n = 3$).

	Z-average size* (nm)	PDI**	Zeta potential (mV)	Encapsulation Efficiency (%)	Drug content (μg/mL)
PLD	96.5 ± 1.5	0.118 ± 0.7	−3.09 ± 0.04	100	2
PLD-50	111.8 ± 0.8	0.046 ± 1.2	−4.06 ± 1.0	91.27 ± 0.8	1.82 ± 0.01
PLD-100	112.3 ± 0.5	0.061 ± 0.3	−2.92 ± 1.3	95.34 ± 2.5	1.91 ± 0.05
PLD-200	112.9 ± 3.1	0.101 ± 0.6	−3.10 ± 0.8	87.5 ± 1.8	1.75 ± 0.04
PLD-400	118.9 ± 1.8	0.135 ± 1.1	−3.46 ± 2.1	90.1 ± 3.4	1.8 ± 0.07

*The size of liposomes (Z-average) ** PDI: polydispersity index.

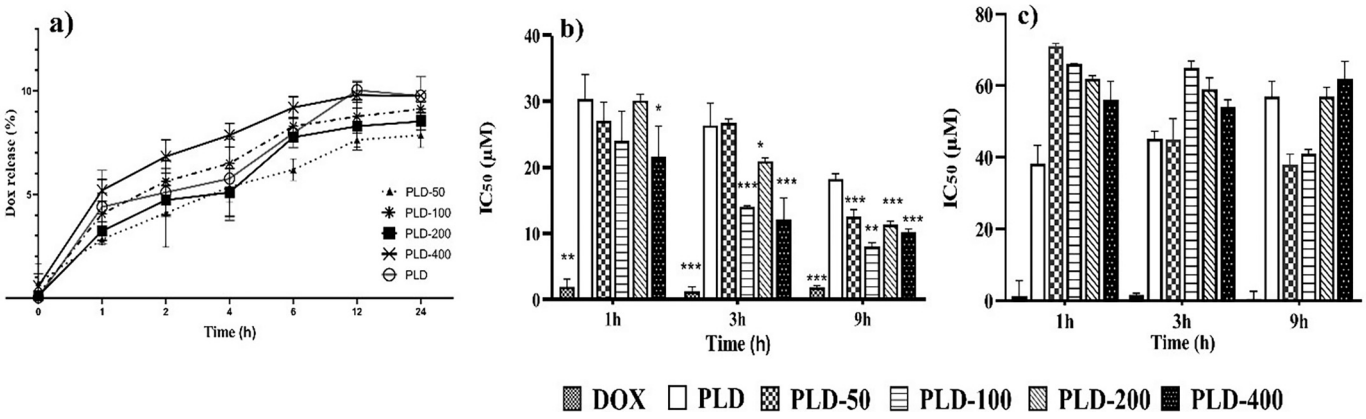

Fig. 3. *In vitro* release profile of Dox from PLD and PLD formulations at pH 7.4 (a). *In vitro* cytotoxic effects against C26 (b) and HUVEC (c) cells. The IC50 was measured by MTT assay after different exposure times. All formulations are compared to PLD. The data are presented as mean ± SD ($n = 3$).

liver and spleen accumulation (Soundararajan et al., 2009). The RES (reticuloendothelial system) effect could be the reason for the elevated concentration of formulations in the liver and spleen. It has been reported that the spleen is responsible for the IgM response before triggering a more persistent immune response. Besides, AR13 peptide has a positive charge (+2) under the acidic environment of the tumor. Due to the optimal affinity toward serum proteins (with a negative charge), these liposomes are more prone to recognition by the Mononuclear phagocytic system (Gyanani et al., 2021). Employing pH/thermos-sensitive liposomes may reduce this effect and increase tumor-targeting efficiency (Pourradi et al., 2022; Aghdam et al., 2019; Chiu et al., 2005).

3.8. Antitumor activity

The antitumor activities of PLD-400 were examined on the C26 mouse model that received a single dose of 15 mg/kg of the drugs.

Tumor volume and body weight of mice are demonstrated in Fig. 6a & b. As illustrated, after 44 days post-tumor inoculation, PLD-400, and PLD group showed significant differences in tumor volume compared to the PBS group. PLD-400 group reduced tumor volume more effectively than PBS and PLD groups. Mice treated with PLD-400 didn't exhibit any significant weight loss, and therefore the formulation had no markedly side effects. Our survival curve (Fig. 6c) clearly shows that on day 44, we had 20% survival in the PLD group and 60% survival in the PLD-400 group. The time to reach endpoint (TTE) for PLD-400 was 44, while it was 29.6 and 38.2 for PBS and PLD groups, respectively. Therefore, PLD-400 improved the survival curve effectively compared with PBS. In the control group, the median survival time (MST) was 30, while it was increased in the PLD-treated group (41) and PLD-400 group (44). Treatment with modified-PLD could prolong MST and improve survival, which was also indicated in other studies (Moosavian et al., 2018). The Percentage of tumor growth delay (TGD%) was 29 for PLD and 37 for the PLD-400 group. These results are correlate with our cytotoxicity and biodistribution analysis, as AR13-PLD was more cytotoxic against C26 cells in the tumor environment than PLD.

Our result is in agreement with our previous study, which reported that modified PLD with a suitable peptide exhibited better survival time compared to the non-modified liposomes. Although AR13 peptide, which was studied here, was more successful in cell binding and cell uptake evaluations, FA12 peptide (previous study) was more effective in survival analysis (prolonged MST) (Biabangard et al., 2022).

This study has the potential to guide studies aimed at understanding the molecular bases of interaction between Muc1 and AR13 peptide and other peptides similar to AR13. Moreover, this research could inform clinical practice associated with liposomal formulations targeting Muc1 on colon or breast cancer cells as these tissues overexpress Muc1. Further toxicological analysis and more clinical studies in other animal models will need to be evaluated in the future.

4. Conclusion

MUC1 is a glycosylated large transmembrane protein overexpressed in the third most common cancer worldwide; colon cancer. This work aimed to employ PEGylated liposomal doxorubicin (PLD), which was modified with a define number of AR13 peptides to actively target Muc1 on colon cancerous cells and improve anticancer efficiency of the anti-cancer drug as well. Tissue biodistribution and antitumor analysis demonstrated that this novel formulation could promote the survival of animals compared to PLD. The results showed that AR13–PLD with optimum ligand density on the surface of liposomes could be a specific targeting ligand against a variety of cancers that overexpress Muc1 receptor.

Code availability

Not applicable.

Ethical approval

In this work, the experimental protocols for the animal study were approved by the Ethics committee of Ferdowsi University of Mashhad

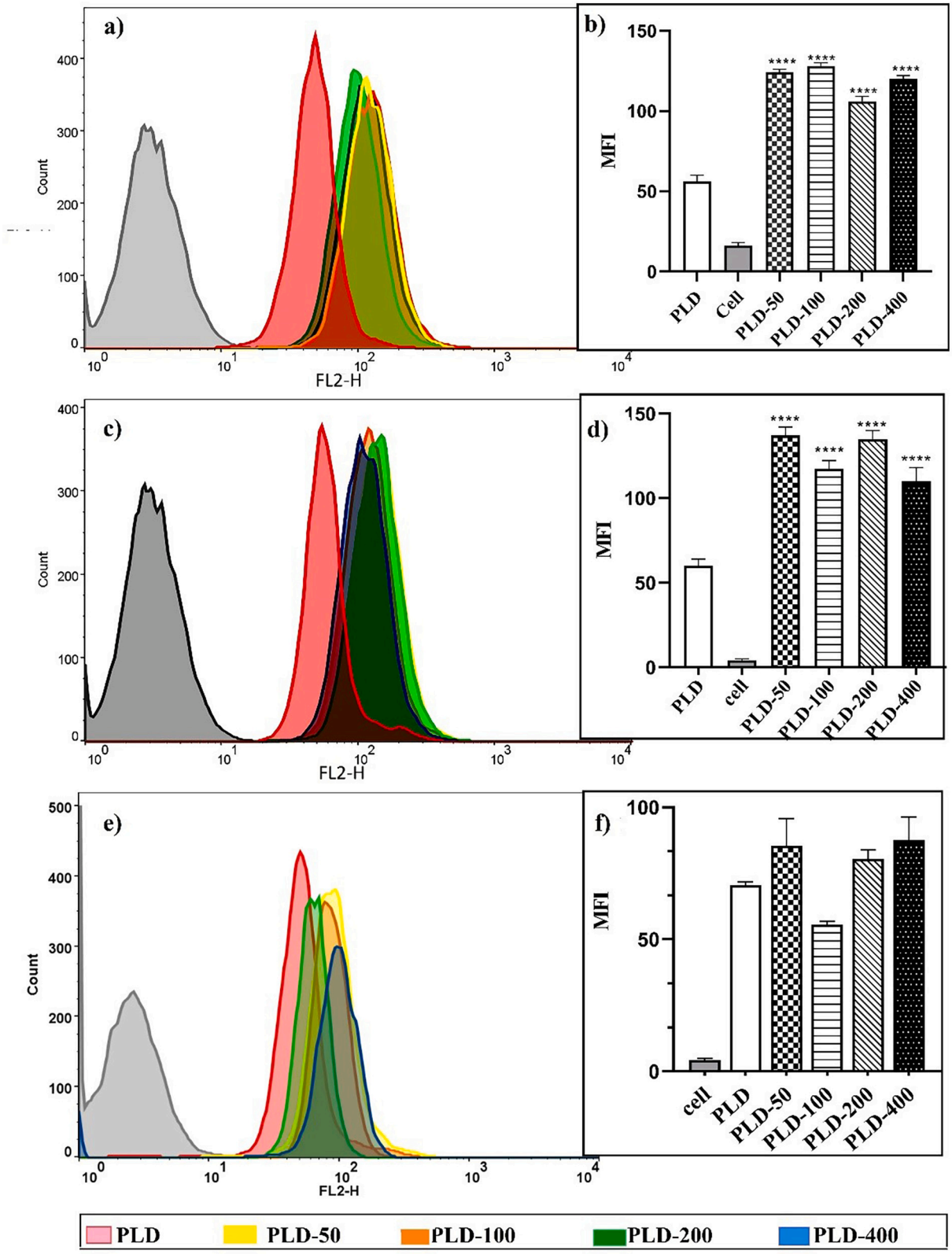

Fig. 4. Cell binding and cell uptake of PLD and AR13-PLD formulations were evaluated at 37 °C and 4 °C. The C26 cell interaction of the formulations at 37 °C (a). The graph demonstrated the mean MFI of formulations at 37 °C (b). The interaction of formulations with C26 cells at 4 °C (c). The MFI of formulations at 4 °C (d). Flow cytometry analysis of C26 cells pretreated with free peptide prior to the addition of different formulations and PLD as the non-targeted control liposome at 37 °C (competition assay) (e). The MFI values of competition assay (f). Data represented as mean ± standard deviation (SEM) (n = 3). ****$p < 0.0001$.

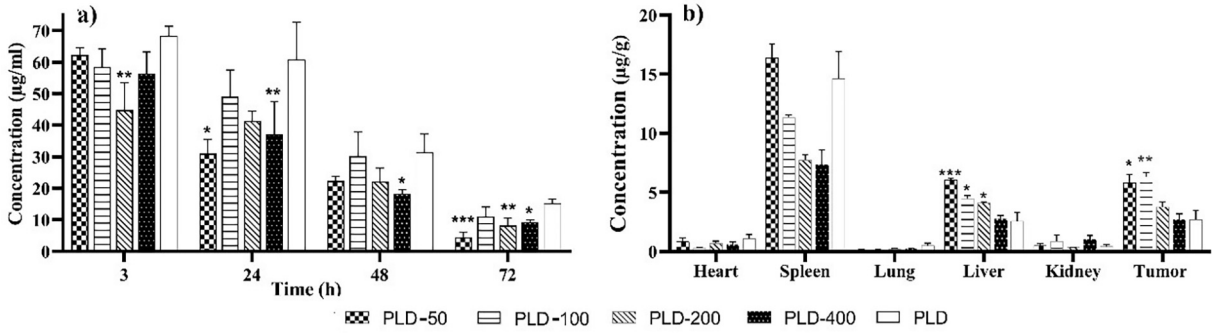

Fig. 5. The distribution of AR13-PLD formulations and PLD at various time points in the blood (a) and in different organs (b) after a single i.v injection of 15 mg/kg liposomal formulations. At 72-h post-injection there were significant differences between formulations and PLD group in blood. Also, after 72 h post injection in tumor, there is a significant difference between PLD and Formulations. PLD is considered the non-targeted control liposome. Data are presented as mean ± SEM. (n = 5 for each group). * p < 0.05, ** p < 0.01 and *** p < 0.001.

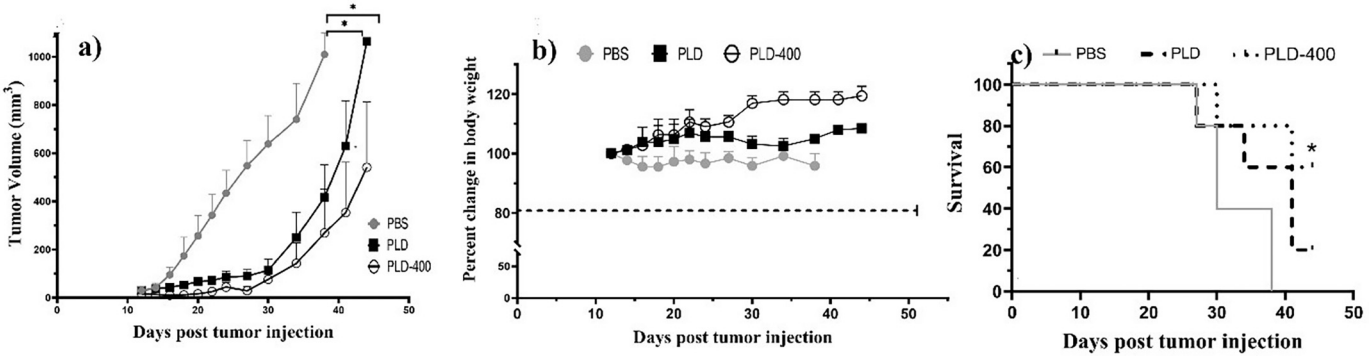

Fig. 6. *In vivo* therapeutic efficacy in female BALB/c mice bearing C26 colon carcinoma tumor after i.v. administration of a single dose of 15 mg/kg liposomal formulations during 44 days. (a) Tumor volume, (b) body weight, and (c) Kaplan–Meier survival curve of different mice groups. PLD-400 group reduced tumor volume and increase survival more effectively than PBS and PLD groups. * represents significant differences of formulations compared to PBS. Data are expressed as means ± SEM (n = 5 per group); * P< 0.05.

(Ethics number: IR.UM.REC.1400.362).

CRediT authorship contribution statement

Atefeh Biabangard: Methodology, Investigation, Software, Writing – review & editing. **Ahmad Asoodeh:** Supervision, Data curation, Project administration. **Mahmoud Reza Jaafari:** Supervision, Conceptualization, Visualization, Project administration. **Fatemeh Moosavi:** Software, Validation.

Declaration of Competing Interest

All authors (A. Biabangard1, A. Asoodeh, M.R. Jaafari, F. Moosavi) declare that they have no conflict of interest.

Data availability

The authors do not have permission to share data.

Acknowledgment

The authors appreciate the support provided by the Research and Technology Council of the Ferdowsi University of Mashhad, Mashhad-Iran (grant number: 3/ 46317, 1396/12/22).

Appendix A. Supplementary data

Supplementary data to this article can be found online at https://doi.org/10.1016/j.taap.2023.116470.

References

Aghdam, Marjan Abri, Bagheri, Roya, Mosafer, Jafar, Baradaran, Behzad, Hashemzaei, Mahmoud, Baghbanzadeh, Amir, de la Guardia, Miguel, Mokhtarzadeh, Ahad, 2019. Recent advances on thermosensitive and pH-sensitive liposomes employed in controlled release. J. Control. Release 315, 1–22.

Agrawal, Babita, Gupta, Nancy, Konowalchuk, Jeffrey D., 2018. MUC1 mucin: a putative regulatory (checkpoint) molecule of T cells. Front. Immunol. 9, 2391.

Alexis, Frank, Pridgen, Eric, Molnar, Linda K., Farokhzad, Omid C., 2008. Factors affecting the clearance and biodistribution of polymeric nanoparticles. Mol. Pharm. 5 (4), 505–515.

Amin, Mohamadreza, Badiee, Ali, Jaafari, Mahmoud Reza, 2013. Improvement of pharmacokinetic and antitumor activity of PEGylated liposomal doxorubicin by targeting with N-methylated cyclic RGD peptide in mice bearing C-26 colon carcinomas. Int. J. Pharm. 458 (2), 324–333.

Arabi, Leila, Badiee, Ali, Mosaffa, Fatemeh, Jaafari, Mahmoud Reza, 2015. Targeting CD44 expressing cancer cells with anti-CD44 monoclonal antibody improves cellular uptake and antitumor efficacy of liposomal doxorubicin. J. Control. Release 220, 275–286.

Asoodeh, Ahmad, Haghighi, Leyla, Chamani, Jamashidkhan, Ansari-Ogholbeyk, Mohamad Amin, Mojallal-Tabatabaei, Zahra, Lagzian, Milad, 2014. Potential angiotensin I converting enzyme inhibitory peptides from gluten hydrolysate: biochemical characterization and molecular docking study. J. Cereal Sci. 60 (1), 92–98.

Barenholz, Yechezkel Chezy, 2012. Doxil®—the first FDA-approved nano-drug: lessons learned. J. Control.Rel. 160 (2), 117–134.

Bartlett, Grant R., 1959. Phosphorus assay in column chromatography. J. Biol. Chem. 234 (3), 466–468.

Biabangard, Atefeh, Asoodeh, Ahmad, Jaafari, Mahmood Reza, Mashreghi, Mohammad, 2022. Study of FA12 peptide-modified PEGylated liposomal doxorubicin (PLD) as an effective ligand to target Muc1 in mice bearing C26 colon carcinoma: in silico, in vitro, and in vivo study. Expert Opin. Drug Deliv. 1-15 https://doi.org/10.1080/17425247.2022.2147505.

Bolat, Zeynep Busra, Nezir, Ayca Ece, Devrim, Burcu, Zemheri, Ebru, Gulyuz, Sevgi, Ozkose, Umut Ugur, Yilmaz, Ozgur, Bozkir, Asuman, Telci, Dilek, Sahin, Fikrettin, 2021. Delivery of doxorubicin loaded P18 conjugated-poly (2-ethyl-oxazoline)-DOPE nanoliposomes for targeted therapy of breast cancer. Toxicol. Appl. Pharmacol. 428, 115671.

Chiu, Gigi N.C., Abraham, Sheela A., Ickenstein, Ludger M., Ng, Rebecca, Karlsson, Göran, Edwards, Katarina, Wasan, Ellen K., Bally, Marcel B., 2005. Encapsulation of doxorubicin into thermosensitive liposomes via complexation with the transition metal manganese. J. Control. Release 104 (2), 271–288.

Clogston, Jeffrey D., Patri, Anil K., 2011. Zeta potential measurement. In: McNeil, S. (Ed.), Characterization of Nanoparticles Intended for Drug Delivery. Methods in Molecular Biology, vol 697. Humana Press. https://doi.org/10.1007/978-1-60327-198-1_6.

Darban, Assaran, Reza, Behzad Shareghi, Asoodeh, Ahmad, Chamani, Jamshidkhan, 2017b. Multi-spectroscopic and molecular modeling studies of interaction between two different angiotensin I converting enzyme inhibitory peptides from gluten hydrolysate and human serum albumin. J. Biomol. Struct. Dyn. 35 (16), 3648–3662.

Darban, Shahrzad Amiri, Badiee, Ali, Jaafari, Mahmoud Reza, 2017a. PNC27 anticancer peptide as targeting ligand significantly improved antitumor efficacy of Doxil in HDM2-expressing cells. Nanomedicine 12 (12), 1475–1490.

Diao, Lu, Tao, Jin, Wang, Yiqi, Ying, Hu, He, Wenfei, 2019. Co-delivery of dihydroartemisinin and HMGB1 siRNA by TAT-modified cationic liposomes through the TLR4 signaling pathway for treatment of lupus nephritis. Int. J. Nanomedicine 14, 8627.

Fukumura, D., Jain, R.K., 2007. Tumor microvasculature and microenvironment: targets for anti-angiogenesis and normalization. Microvasc. Res. 74 (2–3), 72–84. https://doi.org/10.1016/j.mvr.2007.05.003.

Goel, Manish Kumar, Khanna, Pardeep, Kishore, Jugal, 2010. Understanding survival analysis: Kaplan-Meier estimate. Int. J. Ayurveda Res. 1 (4), 274–278. https://doi.org/10.4103/0974-7788.76794.

Gyanani, Vijay, Haley, Jeffrey C., Goswami, Roshan, 2021. Challenges of current anticancer treatment approaches with focus on liposomal drug delivery systems. Pharmaceuticals 14 (9), 835.

Haftcheshmeh, Saeed Mohammadian, Jaafari, Mahmoud Reza, Mashreghi, Mohammad, Mehrabian, Amin, Alavizadeh, Seyedeh Hoda, Zamani, Parvin, Zarqi, Javad, Darvishi, Mohammad Hasan, Gheybi, Fatemeh, 2021. Liposomal doxorubicin targeting mitochondria: a novel formulation to enhance anti-tumor effects of Doxil® in vitro and in vivo. J. Drug Deliv. Sci. Technol. 62, 102351.

Haghiralsadat, Fateme, Amoabediny, Ghasem, Helder, Marco N., Naderinezhad, Samira, Sheikhha, Mohammad Hasan, Forouzanfar, Tymour, Zandieh-Doulabi, Behrouz, 2018. A comprehensive mathematical model of drug release kinetics from nano-liposomes, derived from optimization studies of cationic PEGylated liposomal doxorubicin formulations for drug-gene delivery. Artif. Cells Nanomed. Biotechnol. 46 (1), 169–177.

Hatakeyama, Hiroto, Akita, Hidetaka, Harashima, Hideyoshi, 2013. The polyethyleneglycol dilemma: advantage and disadvantage of PEGylation of liposomes for systemic genes and nucleic acids delivery to tumors. Biol. Pharm. Bull. 36 (6), 892–899.

Hayat, Seyed M.G., Jaafari, Mahmoud R., Hatamipour, Mahdi, Penson, Peter E., Sahebkar, Amirhossein, 2020. Liposome circulation time is prolonged by CD47 coating. Protein Pept. Lett. 27 (10), 1029–1037.

Hernández-Caselles, Trinidad, Villalaín, José, Gómez-Fernández, Juan C., 1993. Influence of liposome charge and composition on their interaction with human blood serum proteins. Mol. Cell. Biochem. 120 (2), 119–126.

Hess, Berk, Bekker, Henk, Berendsen, Herman J.C., Fraaije, Johannes G.E.M., 1997. LINCS: a linear constraint solver for molecular simulations. J. Comput. Chem. 18 (12), 1463–1472.

Iden, Debbie L., Allen, Theresa M., 2001. In vitro and in vivo comparison of immunoliposomes made by conventional coupling techniques with those made by a new post-insertion approach. Biochim. Biophys. Acta Biomembr. 1513 (2), 207–216.

Khondee, Supang, Chittasupho, Chuda, Tima, Singkome, Anuchapreeda, Songyot, 2018. Doxorubicin-loaded micelle targeting MUC1: a potential therapeutic for MUC1 triple negative breast cancer treatment. Curr. Drug Deliv. 15 (3), 406–416.

Kim, Jin-Seok, 2016. Liposomal drug delivery system. J. Pharm. Investig. 46 (4), 387–392. https://doi.org/10.1007/s40005-016-0260-1.

Korani, Mitra, Nikoofal-Sahlabadi, Sara, Nikpoor, Amin R., Ghaffari, Solmaz, Attar, Hossein, Mashreghi, Mohammad, Jaafari, Mahmoud R., 2020. The effect of phase transition temperature on therapeutic efficacy of liposomal bortezomib. Curr. Med. Chem. Anticancer Agents 20 (6), 700–708.

Laskowski, Roman A., Antoon, J., Rullmann, C., MacArthur, Malcolm W., Kaptein, Robert, Thornton, Janet M., 1996. AQUA and PROCHECK-NMR: programs for checking the quality of protein structures solved by NMR. J. Biomol. NMR 8 (4), 477–486.

Lee, Mi-Kyung, 2019. Clinical usefulness of liposomal formulations in cancer therapy: lessons from the experiences of doxorubicin. J. Pharm. Investig. 49 (2), 203–214. https://doi.org/10.1007/s40005-018-0398-0.

Liang, Yanqin, Li, Suxin, Wang, Xueling, Zhang, Yuan, Sun, Yanan, Wang, Yaoqi, Wang, Xiaoyou, He, Bing, Dai, Wenbing, Zhang, Hua, 2018. A comparative study of the antitumor efficacy of peptide-doxorubicin conjugates with different linkers. J. Control. Release 275, 129–141.

Maiti, Sabyasachi, Sen, Kalyan Kumar, 2017. Introductory chapter: drug delivery concepts. Adv. Technol. Deliv. Ther. 1–12.

Mashreghi, Mohammad, Zamani, Parvin, Moosavian, Seyedeh Alia, Jaafari, Mahmoud Reza, 2020. Anti-Epcam aptamer (Syl3c)-functionalized liposome for targeted delivery of doxorubicin: in vitro and in vivo antitumor studies in mice bearing C26 colon carcinoma. Nanoscale Res. Lett. 15 (1), 1–13.

Moosavian, Seyedeh Alia, Abnous, Khalil, Akhtari, Javad, Arabi, Leila, Dewin, Ali Gholamzade, Jafari, Mahmoudreza, 2018. 5TR1 aptamer-PEGylated liposomal doxorubicin enhances cellular uptake and suppresses tumour growth by targeting MUC1 on the surface of cancer cells. Artif. Cells Nanomed. Biotechnol. 46 (8), 2054–2065.

Moreira, João N., Ishida, Tatsuhiro, Gaspar, Rogério, Allen, Theresa M., 2002. Use of the post-insertion technique to insert peptide ligands into pre-formed stealth liposomes with retention of binding activity and cytotoxicity. Pharm. Res. 19 (3), 265–269.

Nagayasu, A., Uchiyama, K., Kiwada, H., 1999. The size of liposomes: a factor which affects their targeting efficiency to tumors and therapeutic activity of liposomal antitumor drugs. Adv. Drug Deliv. Rev. 40 (1–2), 75–87.

Nam, Kwangho, Gao, Jiali, York, Darrin M., 2005. An efficient linear-scaling Ewald method for long-range electrostatic interactions in combined QM/MM calculations. J. Chem. Theory Comput. 1 (1), 2–13.

Neto, Daniel Ferreira, de Lima, Vagner, Fonseca, Ronaldo Jesus, Dutra, Leonardo Hermes, Miranda, Layssa, de Oliveria, Portela, Freitas, Carla, Fillizola, Eduardo, Soares, Breno, de Abreu, André Luiz, Twiari, Sandeep, 2022. Molecular dynamics simulations of the SARS-CoV-2 spike protein and variants of concern: structural evidence for convergent adaptive evolution. J. Biomol. Struct. Dyn. 1–13.

Nikoofal-Sahlabadi, Sara, Riahi, Maryam Matbou, Sadri, Kayvan, Badiee, Ali, Nikpoor, Amin Reza, Jaafari, Mahmoud Reza, 2018. Liposomal CpG-ODN: an in vitro and in vivo study on macrophage subtypes responses, biodistribution and subsequent therapeutic efficacy in mice models of cancers. Eur. J. Pharm. Sci. 119, 159–170.

Nolting, Birte, 2013. Linker technologies for antibody–drug conjugates. Antibody-drug Conjug. 71–100.

Pinheiro, R.G.R., Granja, Andreia, Loureiro, Joana A., Pereira, M.C., Pinheiro, M., Neves, A.R., Reis, S., 2020. RVG29-functionalized lipid nanoparticles for quercetin brain delivery and Alzheimer's disease. Pharm. Res. 37 (7), 1–12.

Pourradi, Nasibeh Mohammad, Ali, Hossein Babaei, Hamishehkar, Hamed, Baradaran, Behzad, Shokouhi-Gogani, Behrooz, Shanehbandi, Dariush, Ghorbani, Marjan, Azarmi, Yadollah, 2022. Targeted delivery of doxorubicin by Thermo/pH-responsive magnetic nanoparticles in a rat model of breast cancer. Toxicol. Appl. Pharmacol. 446, 116036 https://doi.org/10.1016/j.taap.2022.116036. https://www.sciencedirect.com/science/article/pii/S0041008X22001818.

Rajagopalan, Rukkumani, Yakhmi, Jatinder V., 2017. Nanotechnological approaches toward cancer chemotherapy. In: Nanostructures for Cancer Therapy. Chapter 8 - Nanotechnological approaches toward cancer chemotherapy, pp. 211–240.

Ramakrishnan, C., Ramachandran, G.N., 1965. Stereochemical criteria for polypeptide and protein chain conformations: II. Allowed conformations for a pair of peptide units. Biophys. J. 5 (6), 909–933.

Reinhardt, Andre, Neundorf, Ines, 2016. Design and application of antimicrobial peptide conjugates. Int. J. Mol. Sci. 17 (5), 701.

Ryckaert, Jean-Paul, Ciccotti, Giovanni, Berendsen, Herman J.C., 1977. Numerical integration of the cartesian equations of motion of a system with constraints: molecular dynamics of n-alkanes. J. Comput. Phys. 23 (3), 327–341.

Schneidman-Duhovny, Dina, Inbar, Yuval, Nussinov, Ruth, Wolfson, Haim J., 2005. PatchDock and SymmDock: servers for rigid and symmetric docking. Nucleic Acids Res. 33 (suppl_2), W363–W367.

Shahraki, Naghmeh, Mehrabian, Amin, Amiri-Darban, Shahrazad, Moosavian, Seyedeh Alia, Jaafari, Mahmoud Reza, 2021. Preparation and characterization of PEGylated liposomal doxorubicin targeted with leptin-derived peptide and evaluation of their anti-tumor effects, in vitro and in vivo in mice bearing C26 colon carcinoma. Colloids Surf. B: Biointerfaces 200, 111589.

Shi, Xiangyang, Sun, Kai, Baker Jr, James R., 2008. Spontaneous formation of functionalized dendrimer-stabilized gold nanoparticles. J. Phys. Chem. C 112 (22), 8251–8258.

Sonju, Jafrin Jobayer, Dahal, Achyut, Singh, Sitanshu S., Jois, Seetharama D., 2021. Peptide-functionalized liposomes as therapeutic and diagnostic tools for cancer treatment. J. Control. Release 329, 624–644.

Soundararajan, Anuradha, Bao, Ande, Phillips, William T., Ricardo Perez, I.I.I., Goins, Beth A., 2009. [186Re] liposomal doxorubicin (Doxil): in vitro stability, pharmacokinetics, imaging and biodistribution in a head and neck squamous cell carcinoma xenograft model. Nucl. Med. Biol. 36 (5), 515–524.

Subhan, Abdus, Md, Siva Kishan, Satya, Yalamarty, Filipczak, Nina, Parveen, Farzana, Torchilin, Vladimir P., 2021. Recent advances in tumor targeting via EPR effect for cancer treatment. J. Pers. Med 11 (6), 571.

Swope, William C., Pitera, Jed W., Germain, Robert S., 2006. Molecular simulation and systems biology. Netw. Mod. Appl. 67.

Taylor-Papadimitriou, J., Burchell, J., Miles, D.W., Dalziel, M., 1999. MUC1 and cancer. Biochim. Biophys. Acta Mol. basis Dis. 1455 (2–3), 301–313.

Turkbey, Baris, Mani, Haresh, Aras, Omer, Rastinehad, Ardeshir R., Shah, Vijay, Bernardo, Marcelino, Pohida, Thomas, Daar, Dagane, Benjamin, Compton, McKinney, Yolanda L., 2012. Correlation of magnetic resonance imaging tumor volume with histopathology. J. Urol. 188 (4), 1157–1163.

Yoo, Jihye, Park, Changhee, Yi, Gawon, Lee, Donghyun, Koo, Heebeom, 2019. Active targeting strategies using biological ligands for nanoparticle drug delivery systems. Cancers 11 (5), 640.

Zhiping, Zhou, Jianmin, Xu, Xubing, Song, Deyue, Yan, 1992. Calculation of the mean-square radius of gyration for polymer chains with side-groups. Eur. Polym. J. 28 (11), 1339–1343.